

Effect of Post-Weld Heat Treatment on the Corrosion Behavior of Resistance Spot Welded Super Duplex Stainless UNS S 32750

Byung-hyun Shin, Sanghyup Park, Junghyun Park, Dohyung Kim,
Myoungwon Hwang, and Wonsub Chung*

Pusan National University, Department of Materials Science and Engineering, Busan, Korea

*E-mail: wschung1@pusan.ac.kr

Received: 8 October 2018 / Accepted: 3 December 2018 / Published: 7 February 2019

Super duplex stainless steel (SDSS) has high corrosion resistance. However, welding decreases its corrosion resistance due to the segregation of its major constituent elements by excessive ferritization in the weld zone (WZ) of SDSS. Increased welding current at resistance spot welding (RSW) increased the nugget size from 5.3 mm (6.0 kA) to 5.8 mm (8.0 kA), which in turn decreased the corrosion resistance. A larger WZ decreased the active potential (E_{corr}) and increased the active current density (I_{corr}). Welded SDSS specimens exhibited heterogeneous pitting below the pitting potential. Heat treatment for a short time at a high temperature (1200 °C) improved the corrosion resistance by modifying the volume fractions of austenite and ferrite. Heat treatment for 3 min resulted in the highest corrosion resistance, as an equal volume fraction of austenite and ferrite was achieved at this time.

Keywords: Super duplex stainless steel; Resistance spot welding; Welding current; Post-weld heat treatment; Corrosion behavior

1. INTRODUCTION

Duplex stainless steel (DSS) is a dual-phase stainless steel containing both austenite and ferrite [1-3]. DSS combines the high corrosion resistance of austenite and the high strength of ferrite [1-6]. These properties are required in high-pressure and high-corrosion environments, such as those typically found in offshore or chemical refining plants, to prevent the breakdown of steel structure [7-9]. The grade of DSS is determined by its pitting resistance equivalent (PRE = wt.% Cr + 3.3 wt.% Mo + 16 wt.% N); super duplex stainless steel (SDSS) has PRE values ranging from 40 to 50 [1, 2, 9-12].

Resistance welding is most frequently used, because it has the lowest production cost. Welding is an easy manufacturing process for the fabrication of pipes [13-16]. The resistance welding of DSS

has not yet been studied, because welding is known to decrease the corrosion resistance of all structural materials [17-22].

SDSS is composed of austenite and ferrite, and has excellent workability and weldability [17-22]. SDSS is subjected to solution annealing at 1100 °C and quenching to achieve its high corrosion resistance [1, 3, 12]. However, this processing cannot be used with welding because the welding current would be discharged by the water.

Previous studies have evaluated the effect of heat treatment on the corrosion resistance of SDSS. Nilsson studied the effect of heat treatment on the microstructure of SDSS to examine phase changes as a function of temperature [1, 2]. The chemical composition varied as a function of temperature, and changed the corrosion behavior because the change in the PRE made the weaker phase (lower PRE made pitting site) [12]. Chen studied the effect of solution heat treatment (at 1100 °C) on pitting corrosion [3]. Lopes examined the changes in mechanical and corrosion properties with different welding conditions during inert gas welding (Arc welding) [22]. Investigation of the microstructure on the weld zone (WZ) revealed that Wimanstatten and allotriomorphic austenites were formed due to the rapid cooling of the WZ. However, the studies on the ability of heat treatment to improve corrosion resistance after resistance spot welding (RSW) have been not reported.

In order to fabricate SDSS pipes, studies of its weldability and corrosion behavior in resistance welding are required. Arc welding and laser welding was found to decrease the corrosion resistance, due to segregation in the WZ and heat-affected zone (HAZ), which resulted in unfavorable volume fractions of austenite and ferrite [17-22]. But resistance welding is not studied by anyone. Welded SDSS requires the post-weld heat treatment to improve its corrosion resistance.

SDSS is used in harsh high-pressure and high-corrosion industrial environments. WZ show the decreased strength and corrosion resistance due to the changes that occur in their microstructure during the rapid cooling by electrode tip after welding [1-3, 16-18]. Therefore, the WZ in SDSS requires the post-weld heat treatment in order to restore its high strength and high corrosion resistance.

This study investigated the changes in the weldability as function of welding current, and the effect of different post-weld heat treatment durations on the corrosion behavior after resistance spot welding of SDSS. The weldability and corrosion resistance of the welded SDSS were evaluated using the potentiodynamic polarization curve and critical pitting temperature (CPT, potentiostatic test).

2. MATERIALS AND METHODS

The investigated SDSS was commercially manufactured UNS S 32750 plate with 3 mm thickness; its chemical composition is shown in Table 1. The PRE of the material was calculated to be 42, and it contained approximately equal volume fractions of austenite and ferrite (the optimized corrosion resistance) [1, 2, 7-9].

RSW was performed using an inverter DC (Direct current) resistance spot welding machine, and the welding conditions followed the ISO 14373 standard. The electrode force is 4.8 kN, the squeeze time is 1.67 sec, the welding time is 0.47 sec, and the cooling time is 0.47 sec. The welding current was varied from 6.0 kA to 8.5 kA by increasing the current in 0.5 kA increments. The changes in the welding current affected the WZ and HAZ because the heat input energy (1) was changed.

$$Q = I^2Rt \quad (1)$$

Q : heat input energy, I : welding current, R : resistance of material, t : welding time

Post-weld heat treatment was applied for 0 to 10 min at 1200 °C to improve the corrosion resistance caused by the unequal volume fractions of ferrite and austenite in the WZ. SDSS is normally quenched after solution annealing at 1100 °C to optimize the corrosion resistance [1, 3, 12]. However, this procedure cannot be used during welding because the welding current would be discharged by the water.

Table 1. Chemical composition of commercial super duplex stainless steel UNS S 32750

Elements	C	N	Mn	Ni	Cr	Mo	Cu	W	Fe
Concentration (wt. %)	0.014	0.27	0.79	6.8	25.0	3.8	0.18	0.02	Bal

Thus, post-weld heat treatment was performed at 1200 °C, and the sample was subsequently cooled in air.

The welding specimens were cut to examine their microstructure and to conduct corrosion tests. For the electrolysis etching, 50 g NaOH + 450 mL distilled water solution was used. During etching, a potential of 10 V and current of 2.4 A were applied. The microstructure was examined using a field emission scanning electron microscope (FE-SEM, Hitachi S-4800), and the chemical composition of each phase was determined using energy dispersive spectroscopy (EDS). The chemical composition of N could not be analyzed using EDS due to a lack of accuracy; therefore, the values for N were calculated from reference data [12]. Nugget diameter calculated the size of weld zone to check the weldability [20]. The volume fractions of austenite and ferrite on the specimens were measured according to ASTM E 1245.

Potentiodynamic polarization curves and CPT tests were performed to analyze the changes in the corrosion resistance as the welding conditions and the post-weld heat treatment [1-3, 10-12]. A potentiodynamic polarization curve, in which the potential is analyzed as a function of the potential, was used to analyze the corrosion behavior. The potentiodynamic polarization curve was acquired using a three-electrode cell in a 3.5 wt. % NaCl solution by scan rate of 0.167 mV/s. The reference electrode was a saturated calomel electrode (SCE), and the counter electrode was a 20 mm × 20 mm Pt mesh. CPT (potentiostatic test at 700 mV_{SCE}) was used to determine the difference of pitting growth in a 5.85 wt. % NaCl solution. The CPT measurements determined the temperatures, and that is over 100 μA/cm² during a 1 min test. The increasing rate of temperature is 1 °C per min.

3. RESULTS AND DISCUSSION

3.1 Effect of the welding current

After RSW, the microstructure was divided into WZ, HAZ, and BM regions. Fig. 1 shows the microstructure an SDSS sample after welding at 6.0 kA. The WZ showed a high volume fraction of

ferrite, because austenite could not grow during rapid cooling due to the indirect quenching by the electrode tip. The austenite grains in the WZ were fine (size under 5 μm).

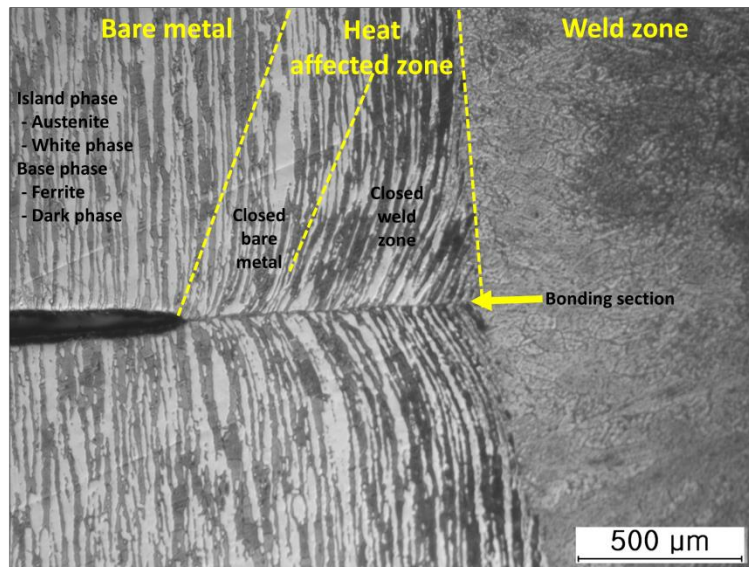


Figure 1. Microstructure of weld zone, heat affected zone and bare metal after resistance spot welding at 6 kA in super duplex stainless steel UNS S 32750

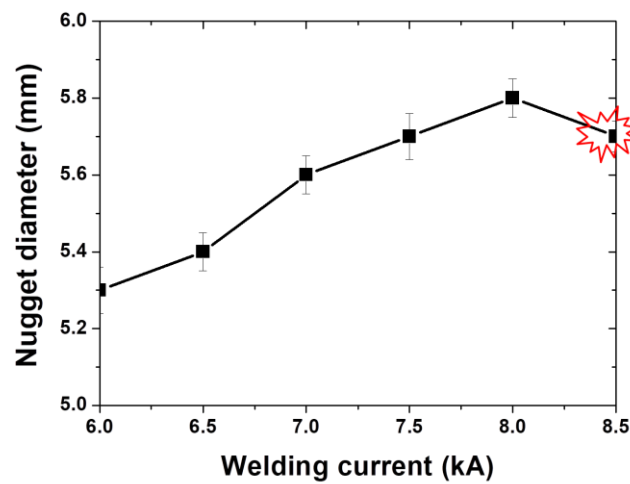


Figure 2. Nugget diameter as a function of the welding current from 6.0 kA to 8.5 kA in super duplex stainless steel UNS S 32750

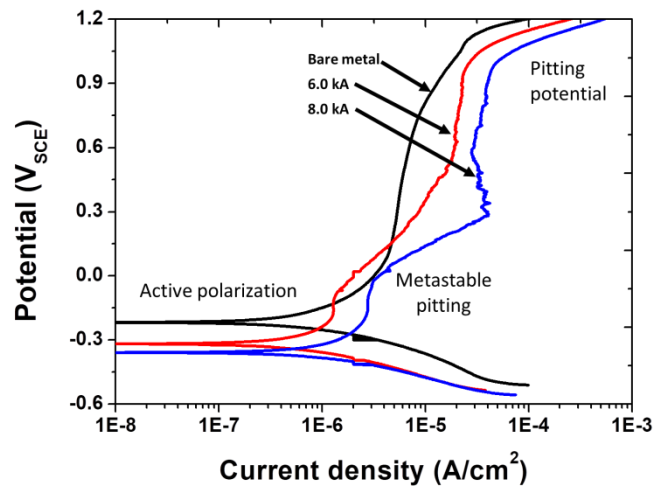


Figure 3. Potentiodynamic polarization curve in 3.5 wt. % NaCl as the welding current of super duplex stainless steel UNS S 32750

Table 2. Key parameters of the potentiodynamic polarization curves as a function of the welding current form 6.0 kA to 8.5 kA: (a) E_{corr}, (b) I_{corr}, (c) metastable pit, and (d) E_{pit}

	Bare	6.0 kA	6.5 kA	7.0 kA	7.5 kA	8.0 kA	8.5 kA
E _{corr} (mV)	- 220 ± 3	- 313 ± 4	- 331 ± 5	- 337 ± 4	- 341 ± 3	- 348 ± 4	- 343 ± 4
I _{corr} (uA/cm ²)	0.2 ± 0.1	0.5 ± 0.1	0.6 ± 0.1	0.7 ± 0.1	0.8 ± 0.1	0.9 ± 0.1	0.8 ± 0.1
Metastable pit (mV)		- 30 ± 2	- 28 ± 3	- 25 ± 2	- 22 ± 2	- 18 ± 3	- 21 ± 2
E _{pit} (mV)	1120 ± 10	1035 ± 3	1033 ± 3	1028 ± 3	1025 ± 3	1020 ± 3	1023 ± 2

That shows no enough cooling time to grow austenite after melting [22]. The temperature of the HAZ can be estimated based on the volume fraction using data from a previous study [14]. The HAZ after RSW could be divided into two types of regions, containing either a high or low volume fraction of austenite. The region with a low volume fraction (under 46 %) of austenite was produced at temperatures above 1200 °C and that was located near the WZ [14]. The region with a high volume fraction (over 54 %) of austenite was produced at temperature above 1050 °C and was located near the BM. The width of the HAZ decreased from 1 mm to 0.5 mm when the electrode tip closed because of the high cooling rate of the electrode tip. The high thermal energy generated at the surface being joined was decreased by the high cooling rate and that decreased the width of HAZ.

Increasing the welding current increased the diameter of WZ of SDSS due to the increased heat input energy ($Q = I^2Rt$). Fig. 2 shows the nugget size as a function of the welding current. The

increased size of WZ as the welding current was increased up to 8.0 kA, but decreased at 8.5 kA due to spatter.

The corrosion behavior as welding currents is shown in Fig. 3. RSW of SDSS showed decreased potential (E_{corr}) and increased current density (I_{corr}) at active polarization. The passivation after active polarization in the potentiodynamic polarization curve of SDSS indicated the effect of resistance welding on corrosion behavior. The key parameters of the potentiodynamic polarization curve as a function of the welding current density are shown in Table 2. The increased volume fraction of ferrite decreased the values of E_{corr} and E_{pit} , because the increased current density increased the size of the low corrosion resistance WZ. The welding made the metastable pitting from -20 to -30 mV_{SCE}.

Table 3. Chemical composition in the weld zone of austenite and ferrite at 6.0 kA after resistance spot welding of super duplex stainless steel UNS S 32750

	Cr	Mo	N	Ni	Fe	PRE
Austenite	25.1 ± 0.3	3.6 ± 0.1	2.05	12.5 ± 0.2	Bal	69.8
Ferrite	25.2 ± 0.2	3.8 ± 0.1	0.05	6.1 ± 0.1	Bal	38.6

Ferritization of the WZ exhibited low corrosion resistance due to the segregation of Cr, Ni, and Mo. Table 3 shows the chemical composition of the WZ; the measured composition was used to determine the PRE in the WZ. A low volume fraction of austenite was observed in the WZ due to the insufficient growth time after RSW. The low corrosion resistance is connected to the difference in the PRE values of austenite and ferrite (PRE gap = 31.2). Ferrite of low PRE became the weaker phase. WZ made metastable pit because of heterogeneous austenite.

3.2 Effect of post-weld heat treatment on microstructure

Post-weld heat treatment was found to improve the corrosion resistance of the SDSS. The SEM images in Fig. 4 show the microstructure of the WZ as a function of heat treatment time at 1200 °C. Increased heat treatment time resulted in larger austenite grains and a greater volume fraction of austenite. The volume fraction is shown in Fig. 5, and the calculated number of austenite grains in a 100 μm^2 area is shown in Fig. 6 as a function of heat treatment time. The austenite grains became coarser, with the number of austenite grains decreasing from 1.36 pcs to 0.32 pcs per 100 μm^2 by the heat treatment at 10 min. The grain area of austenite (2) was converted to a volume fraction and grain number using the following relationship:

$$\text{Austenite area } (\mu\text{m}^2) = \text{average grain area of austenite } (\mu\text{m}^2) \times \text{volume fraction of austenite } (\%) \quad (2)$$

The austenite grain area at 0 min was 8.3 μm^2 (2.9 μm diameter), and at 10 min was 144.9 μm^2 (12.0 μm diameter).

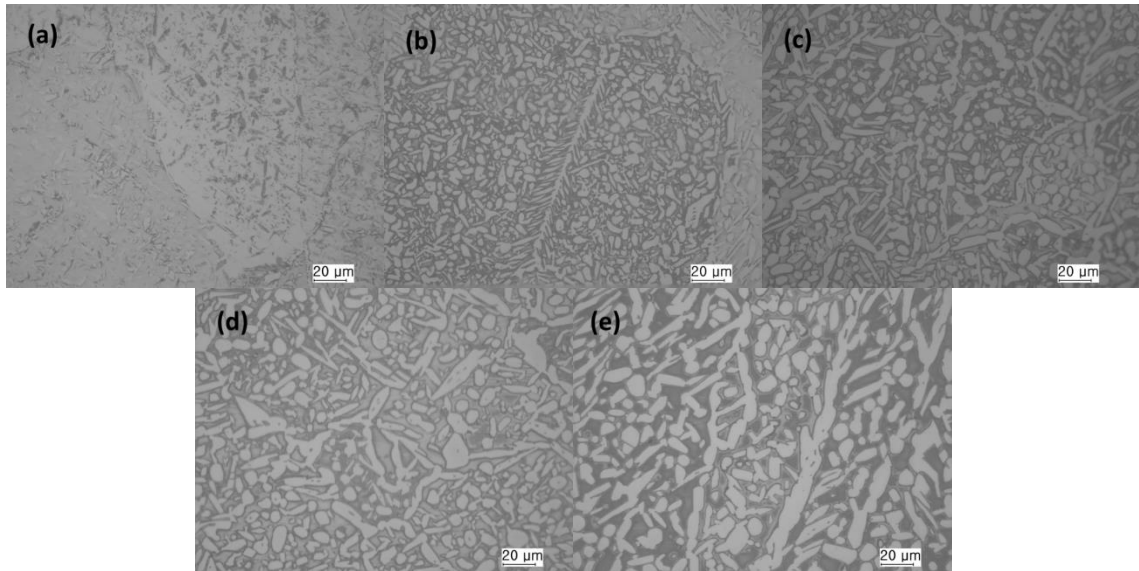


Figure 4. Microstructure of weld zone as a function of post-weld heat treatment time at 1200 °C at 6.0 kA of resistance spot welded super duplex stainless steel UNS S 32750: (a) as-welded, (b) 1 min, (c) 3 min, (d) 5 min, and (e) 10 min

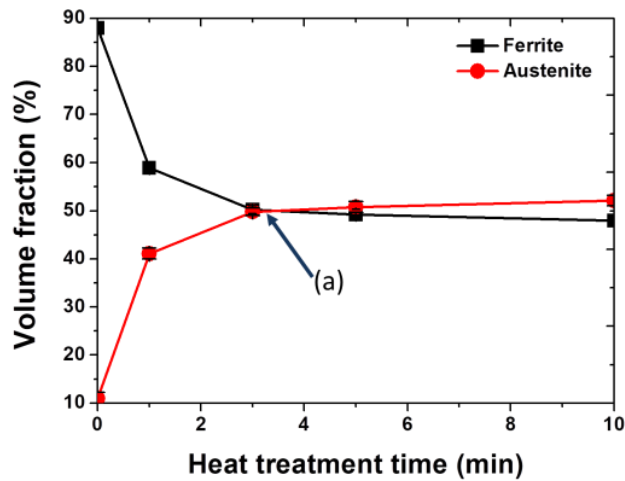


Figure 5. Volume fraction of austenite and ferrite as a function of post-weld heat treatment time at 1200 °C after resistance spot welded super duplex stainless steel UNS S 32750

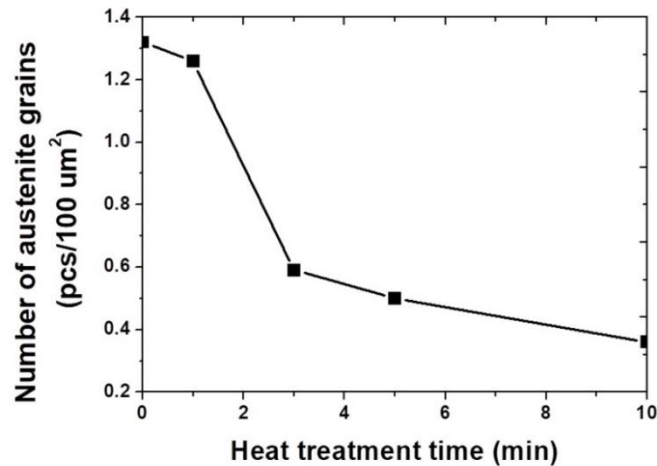


Figure 6. Number of austenite grains in the weld zone as a function of heat treatment time at 1200 °C after resistance spot welded super duplex stainless steel UNS S 32750

The microstructure of WZ had high energy because of residual stress by the quenched microstructure after melting [20, 22].

3.3 Effect of post-weld heat treatment on corrosion

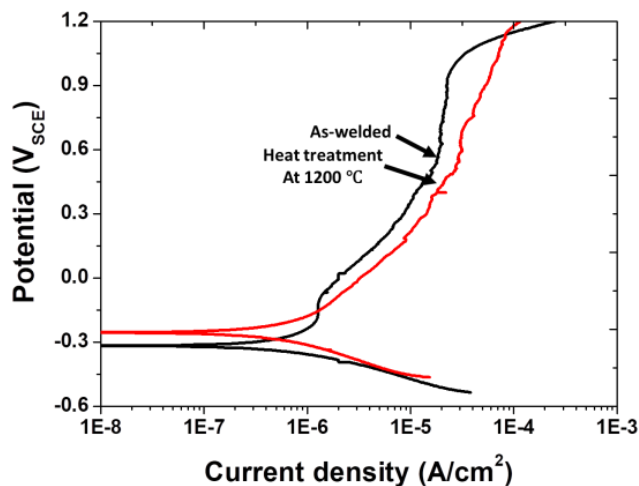


Figure 7. Potentiodynamic polarization curves in 3.5 wt. % NaCl with and without heat treatment at 1200 °C after resistance spot welded super duplex stainless steel UNS S 32750

The microstructure and the volume fraction of austenite in the welded SDSS changed with the heat treatment time. The corrosion behavior of welded SDSS with and without heat treatment is shown in Fig. 7, and the key parameters of the potentiodynamic polarization curve as function of heat treatment time are shown Table 4. These figures illustrate the effect of heat treatment time on the corrosion resistance of welded SDSS. The corrosion resistance of the welded SDSS increased with increasing heat treatment time up to 3 min, and decreased thereafter. The corrosion resistance of SDSS

was affected by the chemical composition of each phase and was a function of the heat treatment time at 1200 °C, as shown in Table 5.

Table 4. Key parameters of the potentiodynamic polarization curve in 35. wt. % NaCl as a function of post-weld heat treatment time: (a) E_{corr} , (b) I_{corr} , (c) metastable pitting potential, and (d) E_{pit}

	As-welded (6.0 kA)	1 min	3 min	5 min	10 min
E_{corr} (mV)	- 313 ± 4	- 295 ± 4	- 255 ± 3	- 285 ± 4	- 288 ± 3
I_{corr} (uA/cm ²)	0.5 ± 0.015	0.4 ± 0.012	0.2 ± 0.011	0.3 ± 0.012	0.3 ± 0.013
Metastable pit (mV)	- 30 ± 10	- 20 ± 10	00 ± 10	- 20 ± 10	- 20 ± 10
E_{pit} (mV)	1020 ± 4	1045 ± 4	1105 ± 5	1084 ± 4	1073 ± 5

Table 5. Chemical composition of austenite and ferrite at the weld zone as a function of heat treatment time at 1200 °C at 6.0 kA in resistance spot welded super duplex stainless steel UNS S 32750

Temperature	Phase	Cr	Mo	Ni	N	PRE
0 min	Austenite	25.1 ± 0.3	3.6 ± 0.1	12.5 ± 0.2	2.05	69.8
	Ferrite	25.2 ± 0.2	3.8 ± 0.1	6.1 ± 0.1	0.05	38.6
1 min	Austenite	24.3 ± 0.2	3.0 ± 0.1	7.4 ± 0.3	0.54	42.8
	Ferrite	26.0 ± 0.4	4.4 ± 0.1	6.3 ± 0.2	0.05	41.3
3 min	Austenite	24.1 ± 0.2	3.0 ± 0.1	7.2 ± 0.1	0.47	41.9
	Ferrite	26.3 ± 0.3	4.6 ± 0.1	6.4 ± 0.2	0.05	42.3
5 min	Austenite	24.0 ± 0.3	2.8 ± 0.1	7.2 ± 0.1	0.47	40.9
	Ferrite	26.4 ± 0.3	4.8 ± 0.1	6.5 ± 0.2	0.05	43.1
10 min	Austenite	23.9 ± 0.3	2.8 ± 0.1	7.1 ± 0.2	0.47	40.5
	Ferrite	26.6 ± 0.4	4.9 ± 0.1	6.5 ± 0.2	0.05	43.6

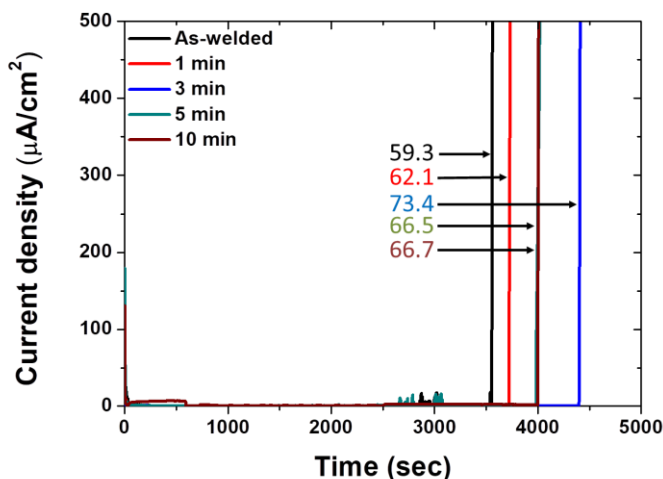


Figure 8. Current density as function of time at 700 mV_{SCE} in 5.85 wt. % NaCl after post-weld heat treatment time at 1200 °C of super duplex stainless steel UNS S 32750

The PRE of the austenite phase that was highest immediately after welding. The post-weld heat treatment decreased the austenite PRE value [3, 4]. In contrast, the PRE of ferrite increased with increasing heat treatment time. The low PRE value in the WZ caused pitting corrosion in the weaker phase [3, 12, 22].

The pitting resistance of SDSS was calculated based on the CPT test, which indicates the temperature at which the passivation layer is destroyed. Fig. 8 shows the current density as a function of time at 700 mV_{SCE} in a 5.85 wt.% NaCl solution. The post-weld heat treatment had an effect on the CPT; the CPT increased as the heat treatment time was increased to 3 min and decreased thereafter. The CPT is related to the growth of the weaker phase, i.e., the phase with a lower PRE [5]. Pitting occurred in ferrite that had undergone 0 to 3 min of heat treatment, while samples that had undergone more than 3 min of heat treatment showed the pitting of austenite. The pitting site changed from ferrite to austenite as the heat treatment progressed because the relative PRE in ferrite and austenite were reversed.

Post-weld heat treatment at 1200 °C after RSW of SDSS changed the corrosion resistance, because the exposure to this high temperature modified the chemical composition of the austenite and ferrite. The corrosion resistance of the welded SDSS was highest after 3 min of heat treatment lasts at 1200 °C, as the heat treated SDSS contained equal volume fractions of austenite and ferrite. Heat treatment at 1200 °C for 10 min resulted in coarse austenite grains (12 μm diameter), and lower corrosion resistance of austenite due to the lower PRE of austenite more than ferrite [8].

Heat treatment of SDSS made the changed corrosion resistance by diffusion of Cr and Mo et al [3, 4]. Corrosion behavior after post-weld heat treatment of resistance spot welded SDSS shows the same results due to same effect of heat treatment [21]. The transformation of microstructure of WZ from ferrite to austenite requires the low energy because that needs low heat treatment time more than casted SDSS [3, 21]. The corrosion resistance of WZ in SDSS is improved to heat treatment by short time of 3 min because WZ had high energy to easy the phase transformation by ferritization.

4. CONCLUSIONS

This study examined the effect of the RSW current and the duration of post-weld heat treatment on the corrosion behavior of SDSS as determined from its potentiodynamic polarization curve.

The WZ of RSW on SDSS contains a high volume fraction of ferrite (over 85%) because of the high cooling rate after melting. The HAZ is divided into a high-temperature HAZ (less than 46% austenite) and a low-temperature HAZ (more than 54% austenite). Increasing the welding current increased the WZ size from 5.3 mm (6.0 kA) to 5.8 mm (8.0 kA), and decreased the corrosion resistance because of chemical composition segregation of ferrite.

The WZ in SDSS has low corrosion resistance (ferrite PRE = 38.6) due to the segregation resulting from the high cooling rate, while austenite has high corrosion resistance (PRE = 69.8). The PRE gap between austenite and ferrite resulted in low corrosion resistance, because pitting occurs in the phase with the lower PRE (weaker phase).

When the duration of the post-weld heat treatment at 1200 °C was increased, the austenite in the WZ became coarser. The CPT value increased with the increasing heat treatment time up to 3 min, due to the crossover of the PRE of austenite and ferrite; the austenite and ferrite had equal PRE values at the crossover point. The post-weld heat treatment of SDSS was increased the corrosion resistance by heat treatment of 3 min at 1200 °C but the heat treatment time over 3 min decreased CPT because of decreased PRE of austenite.

ACKNOWLEDGEMENTS

NRF-2016R1D1A1B04935380

References

1. J.H. Kim, S. W. Choi, D.H. Park, J.M. Lee, *Mater Des.*, 65 (2015) 914
2. J.I. Jang, J. B. Ju, B. W. Lee, D. Kown, W. S. Kim, *Mater Sci Eng A*, 340 (2003) 68
3. J. O. Nilsson, A. Wilson, *J. Mater. Sci. Technol.*, 9 (1993) 545
4. J. O. Nilsson, *J. Mater. Sci. Technol.*, 8 (1992) 685
5. T. H. Chen, J. R. Yang, *Mat. Sci. Eng. A-Struct.*, 311 (2001) 28
6. C. J. Park, V. S. Rao, H. S. Kwon, *Corrosion*, 61 (2005) 76
7. F. Iacoviello, F. Casari, S. Gialanella, *Corros. Sci.*, 47 (2005) 909
8. T.H. Chen, K. L. Weng, J. R. Yan, *Mat. Sci. Eng. A-Struct.*, 338 (2002) 259
9. M. Pohl, O. Storz, T. Glogowski, *Mater. Charact.*, 58 (2007) 65
10. C. P. Dias, O. Balancin, *Metal. Mater. Trans. A*, 62 (2016) 155
11. M. Martins, L. C. Casteletti, *Mater. Charact.*, 60 (2009) 150
12. J. M. Pardal, S. S. M. Tavares, M. C. Fonseca, J.A. de Souzaa, R.R.A. Côrtea, H.F.G. de Abreu, *Mater. Charact.*, 60 (2009) 165
13. E. Angelini, B. D. Benedetti, F. Rosalbino, *Corros. Sci.*, 46 (2004) 1351
14. H. Tan, Y. Jiang, B. Deng, T. Sun, J. Xu, J. Li, *Mater. Charact.*, 60 (2009) 1049
15. Z. Wei, J. Laizhu, H. Jincheng, S. Hongmei, *Mater. Charact.*, 60 (2009) 50
16. N. J. Laycock, M. H. Moayed, R. C. Newman, *J. Electrochem. Soc.*, 145 (1998) 2622
17. M. B. Davanageri, N. S, R. Kadoli, *AJMS*, 5 (2015) 48
18. J. L. Garin, R. L. Mannheim, *International Centre for Diffraction Data*, (2012) 98

19. M. Youselish, M shamanian, A. Saatchi, *J Alloys Compd.*, 509 (2011) 782
20. S.S.M. Travares, J.M. Pardal, L.D. Lima, I.N. Bastos, A.M. Nascimento, J.A. de Souza, *Mater Charact.*, 58 (2007) 610
21. B.H. Shin, J.H. Park, J.B. Jeon, S.B. Heo, W.S. Chung, *Anti-Corros Method M*, 65 (2018) 492
22. S. Wang, Q. Ma, Y. Li, *Mater Des.*, 32 (2011) 831

© 2019 The Authors. Published by ESG (www.electrochemsci.org). This article is an open access article distributed under the terms and conditions of the Creative Commons Attribution license (<http://creativecommons.org/licenses/by/4.0/>).